Intermittent sea–level acceleration

M. Olivieri[a,*], G. Spada[b]

[a] *Istituto Nazionale di Geofisica e Vulcanologia, Sezione di Bologna, via Donato Creti 12, 40128 Bologna, Italy*
[b] *Dipartimento di Scienze di Base e Fondamenti (DiSBeF), Università di Urbino "Carlo Bo", Urbino, Italy*

Abstract

Using instrumental observations from the Permanent Service for Mean Sea Level (PSMSL), we provide a new assessment of the global sea–level acceleration for the last $\sim$ 2 centuries (1820–2010). Our results, obtained by a stack of tide gauge time series, confirm the existence of a global sea–level acceleration (GSLA) and, coherently with independent assessments so far, they point to a value close to 0.01 mm/yr^2. However, differently from previous studies, we discuss how change points or abrupt inflections in individual sea–level time series have contributed to the GSLA. Our analysis, based on methods borrowed from econometrics, suggests the existence of two distinct driving mechanisms for the GSLA, both involving a minority of tide gauges globally. The first effectively implies a gradual increase in the rate of sea–level rise at individual tide gauges, while the second is manifest through a sequence of catastrophic variations of the sea–level trend. These occurred intermittently since the end of the 19th century and became more frequent during the last four decades.

Keywords: *Sea level rise, Sea level acceleration, Tide gauge observations*

1. Introduction

In view of their impact on coastal hazard and society, the problems of secular sea–level rise and of future sea–level trends are the subjects of extensive research (see e.g. Bindoff et al. 2007, Rahmstorf 2007, Cazenave and Remy 2011). There is now a general agreement about the global mean sea–level rise (GMSLR) that occurred during the 20^{th} century (see Table 1 of Spada and Galassi 2012). However, two related climate issues are still debated. The first is the amplitude of the global sea–level acceleration (GSLA) observed during the last centuries and the second is the possible existence of "change points" or "times of inflection" in global reconstructions or in individual tide gauge (TG) records, possibly corresponding to regime shifts of sea–level change. The importance of these issues, both on a regional and on a global perspective, are discussed in the review by Woodworth et al. (2009).

In a seminal work, Douglas (1992) estimated the GSLA by averaging the sea–level accelerations obtained from individual records of globally distributed TGs. GSLA is defined as twice the quadratic term in a polynomial regression within a limited span of time (henceforth, specific values of GSLA and their uncertainty will be simply denoted by a and Δa, respectively). The approach of Douglas (1992), similar to that adopted by Douglas (1991) to estimate the secular GMSLR, only provided weak evidence in support to a GSLA, even for the longest period considered (namely $a \pm \Delta a = (0.001 \pm 0.008)$ mm/yr^2 during 1850–1991). This neatly

*Corresponding author
Email addresses: marco.olivieri@bo.ingv.it (M. Olivieri), giorgio.spada@gmail.com (G. Spada)

contrasted with the significant GSLA predicted to accompany greenhouse warming. The negative result of Douglas (1992) confirmed that of Woodworth (1990), who limited his attention to European records. No acceleration was observed also by Wenzel and Schröter (2010). They reconstructed mean sea level from TGs data (1900–2006) using neural networks although the dataset was then restricted to the period 1950–2006 to prevent the drastic reduction of available data during the first half of the century.

Recent studies, either based on the "virtual station" stacking method (Jevrejeva et al., 2006, 2008) or on a sea–level reconstruction of long TG records (Church and White, 2006, 2011), unanimously point to the existence of a GSLA. Based on a $\sim$ 300–years long time series (1700–2002) obtained by combining short and long TG records, Jevrejeva et al. (2008) reported a GSLA of about $a = 0.01$ mm/yr^2 (the uncertainty was not quantified), which apparently started at the end of the 18^{th} century. The Empirical Orthogonal Function (EOF) approach of Church and White (2006), combined with polynomial regression, suggested GSLA of (0.013 ± 0.006) mm/yr^2 in the period 1870–2001 and of (0.008 ± 0.008) mm/yr^2 when the 20^{th} century only is considered. In the follow–up paper of Church and White (2011), the acceleration (0.009 ± 0.003) mm/yr^2 has been proposed for the time period 1880–2009. Sea–level curves previously presented in the literature or obtained in this study are shown in Fig. 1. F1

The spread of previous GSLA estimates based on tide gauge (TG) records, summarized in Table 1, is significant. The large energy of decadal T1 sea–level fluctuations (Jevrejeva et al., 2006; Chambers et al., 2012; Houston and Dean, 2013), the poor geographical coverage of TGs, the limited number of TGs facing the open seas (hence less affected by coastal processes), and the oceans response to regional changes in the pattern of wind stress (Merrifield, 2011; Sturges and Douglas, 2011; Bromirski et al., 2011) are main causes of uncertainty and potential sources of misinterpretation (see also the discussion in Douglas 1992 and Sturges and Hong 2001). As recently evidenced by Gehrels and Woodworth (2013) and by a number of previous studies, the proposed GSLA value is strongly sensitive to the time span of the instrumental record considered and to additional selection criteria based on the quality of the data set. Spurious effects from gappy time series (Wenzel and Schröter, 2010), contaminating tectonic (e.g. Larsen et al. 2003, Olivieri et al. 2013) or anthropogenic factors (Carbognin et al., 2010) act to further complicate the determination of GSLA.

The constant acceleration model for sea–level rise is appealingly simple and constitutes the most obvious generalization of linear models ($a = 0$) extensively employed to estimate GMSLR since the early determination of Gutenberg (1941) (for a review, see Spada and Galassi 2012). However, inspection of sea–level compilations (Gehrels and Woodworth, 2013) and of individual records (see e.g. Bromirski et al. 2011), also reveal short–lived accelerations and abrupt steepness variations. These can be modeled, to a first approximation, as change points (CPs) separating periods of constant rate and/or of constant acceleration. As pointed by Church and White (2006), a CP model including an abrupt slope change at year ~ 1930, unexpectedly during a period of little volcanic activity, can indeed be invoked as a possible alternative to a constant acceleration model for the time period 1870–2001. Inflections in global and regional compilations of instrumental records at year ~ 1930 have also been proposed by Jevrejeva et al. (2008), Woodworth et al. (2009) and Church and White (2011). Based on proxy and instrumental observations from seven sites, Gehrels and Woodworth (2013) have recently proposed that year 1925 (± 20) could mark the date when sea–level rise started to exceed the long–term Holocene background rate. Inflections or CPs occurring during the 19^{th} century could be more difficult to ascertain in view of the limited amount and sparsity of instrumental data available for that epoch. However, a major acceleration episode has been evidenced by Jevrejeva et al. (2006) during 1850–1870, though its significance was disputed.

Here we provide a new assessment of GSLA based on instrumental (TG) data alone, for the time period 1820–2010. Assuming a constant acceleration model, from a cumulative sea–level curve constructed by TG time series of sufficient length, we obtain GSLA values that are generally consistent with earlier estimates. However, by simple statistical methods, we address in a systematic manner the important role played by non–synchronous CPs at individual TGs in the assessment of the GSLA. Section 2 is devoted to the construction and to the analysis of a global sea–level curve. The results are then discussed in Section 3.

2. Results

2.1. Building a global sea–level curve

In Fig. 1, curves (a) and (b) reproduce the sea–level time series constructed and studied by Jevrejeva et al. (2006) and by Church and White (2006), respectively. The corresponding GSLA values are given in Table 1. The figure also shows an additional curve (c) that we have built by a global stacking of the 315 Revised Local Reference (RLR) annual time series with length $\geq$ 50 yrs, currently available from the Permanent Service for Mean Sea Level (PSMSL) for the time period 1810–2010 (Woodworth and Player, 2003). It is important to note that we did not apply any low–pass filter to the selected time series in order to remove multi–decadal fluctuations, as done by e.g. Jevrejeva et al. (2008). This is motivated by the minimum length of the time series employed here, which corresponds to the absolute minimum of sea–level record length required to avoid contamination by low–frequency variations of sea–level (see Fig. 3 of Douglas 1992 and Jevrejeva et al. 2008). We note, however, that Houston and Dean (2013) have recently contested this view, proposing that for time series shorter than 60 years decadal variations significantly affect estimates of underlying accelerations. Furthermore, we did not attempt to remove *a priori* from the analysis those TG stations which could be possibly affected by tectonic movements and particularly those from Japan, which are indeed numerous (Jevrejeva et al. 2008). As discussed below, the GSLA results obtained here are largely unaffected by the elimination of stations in tectonically active areas. The geographical distribution of the 315 stations employed in this study is shown in Fig. 2a (see also the supplementary kml file). F2a

The stacked sea–level curve (c) in Fig. 1, hereafter referred to as ST curve, has been obtained by computing the average

$$\mathrm{SL}(t_i) = \frac{1}{N(t_i)} \sum_{j=1}^{N(t_i)} \left(\mathrm{sl}_j(t_i) - \mathrm{GIA}_j(t_i) - \overline{\mathrm{sl}}_j \right), \tag{1}$$

where $\mathrm{SL}(t_i)$ is sea–level at the year $t = t_i$ and $N(t_i)$ is the number of TGs for which a value of annual mean sea–level is available. The three terms on the right–hand side of Eq. (1) represent sea–level observed from the j–th TG at time t_i, the glacial isostatic adjustment (GIA) correction for the j–th

TG, and the average sea–level observed during the whole time span during which the TG has been operating, respectively (note that the subtraction of $\overline{\mathrm{sl}}_j$ has no influence on the assessment of GSLA). The range of uncertainty of the global sea–level curve (1) is evaluated by twice the standard deviation $\mathrm{SLD}(t_i)$ around $\mathrm{SL}(t_i)$. Since the computed value of $\mathrm{SLD}(t_i)$ largely exceeds the error on the annual mean from individual stations, which can be estimated at the level of 0.5 mm (Fabio Raichich, personal communication, 2013), this latter is not taken into account in the assessment of the uncertainty associated with curve ST and with other global or individual time series considered in the following. In building the stack (1) only years with $N(t_i) \geq 2$ are considered. The GIA correction has been performed adopting model ICE–5G(VM2) of Peltier (2004) by means of an improved version of program SELEN (Spada et al., 2012), originally proposed by Spada and Stocchi (2007). Possible uncertainties on $\mathrm{GIA}_j(t_i)$ have not been taken into account.

The stacking technique is commonly employed in seismic data processing in order to increase the signal–to–noise ratio and to enhance the coherency of time series (see e.g. Gilbert and Dziewonski 1975). We are aware that the conventional un–weighted stacking (Eq. 1) is not always satisfactory and better results can be obtained using more sophisticated averaging techniques (Liu et al., 2009). However, our elementary approach to the construction of a global sea–level curve is motivated, *a–posteriori*, by the consistency of the GSLA obtained in this way with previous independently derived estimates.

Using bootstrapping (Efron and Tibshirani, 1986), we have determined the best–fitting quadratic polynomial for curve ST, which reads:

$$\mathrm{SL}(t) = (0.0049 \pm 0.0012)\ t^2 + p_1(t), \tag{2}$$

where $\mathrm{SL}(t)$ is expressed in mm and t in years, and $p_1(t)$ is a degree one polynomial whose coefficients are not of concern here. The uncertainty on the quadratic term corresponds to the rms of the distribution of $5,000$ quadratic terms obtained by synthetic curves where $\mathrm{SL}(t_i)$ is taken randomly from a Gaussian deviate with standard deviation $2\mathrm{SLD}(t_i)$. The GSLA implied in (2), i.e. twice the quadratic term, is (0.0098 ± 0.0023) mm/yr^2, where the uncertainty corresponds to the 95% confidence interval, as in Church and White (2006) (here and in the following, we round off to two significant figures in the GSLA uncertainty when the leading digit is 1 or 2, see e.g. Taylor 1997).

Despite the crude averaging implied in Eq. (1), result (2) is generally coherent with previous findings and constitutes an independent confirmation of the existence of a GSLA. In particular, our estimate well matches the value $a \sim 0.01$ mm/yr^2 proposed by Jevrejeva et al. (2008). Since an estimate of the associated uncertainty is not provided by Jevrejeva et al. (2008), we have applied the bootstrapping procedure to their original data. This gives $\Delta a = 0.002$ mm/yr^2, in close agreement with our estimate above based on stacking. This result, however, should be taken cautiously in view of the significantly longer record considered by Jevrejeva et al. (2008) and the larger number of TGs utilized (1023 stations versus the 315 employed here). While the agreement of our result with Church and White (2006) (i.e. $a = 0.013 \pm 0.006$ mm/yr^2) is satisfactory, we note that our GSLA estimate above turns out to be more precise (the fractional uncertainty is $\Delta a/a \sim 20\%$) than in Church and White (2006) (fractional uncertainty $\sim 50\%$). Since the two methods and the two TG sets employed differ, the origin of this discrepancy is difficult to assess. This, of course, also holds for the overall accuracy of our estimate. It is expected that the record length plays a major role in increasing the uncertainty of the assessment. We could verify that when the ST curve is restricted to the same time period (1870–2001) considered by Church and White (2006), the fractional uncertainty increases to $\sim 50\%$.

To evaluate the impact of the number of TGs employed in the GSLA assessment and the related selection criteria, in Fig. 1 we show two further synthetic sea–level curves obtained by Eq. (1). The first (curve d) has been constructed using the global set of 23 TGs considered in the GMSLR assessment of Douglas (1997) henceforth referred to as D97 set, while the second (curve e) includes the 22 TGs recently employed in the study by Spada and Galassi 2012, herein referred to as SG01 TG set. These two global sets, which are partly overlapping, have been determined imposing specific constraints to the length and to the quality of the TG time series (D97) and, in addition, requiring that the GMSLR estimate is essentially independent upon the GIA correction adopted (SG01). We remark that TG stations which could be possibly affected by tectonic movements are expunged *a priori* from these two sets. The bootstrapping procedure provides, for the two sets, consistent GSLA estimates, namely (0.012 ± 0.002) mm/yr^2 and (0.013 ± 0.002) mm/yr^2, respectively. These agree with the results based on the ST curve and with previous estimates in Table 1. This finding supports the idea that, similarly to GMSLR, GSLA can be detected even using a limited number of TGs, provided that their spatial coverage is sufficient and rigorous selection criteria are imposed. This is only apparently in contradiction with the seminal work of Douglas (1992), who effectively imposed these criteria. His negative result with respect to the existence of a GSLA was likely due to the shorter time series compared to those available nowadays.

2.2. Analysis of the sea–level curve ST

In Fig. 3, curve ST is studied more in detail. Red dotted lines above and below the curve correspond to one standard deviation SLD(t_i). Since the number of TGs operating every year $N(t_i)$ varies considerably with t_i (the dependence is displayed in the bottom part of Fig. 3), $SLD(t_i)$ is markedly time dependent. This feature, which also characterizes the reconstructions of Jevrejeva et al. (2008) and reflects the non–stationarity of the time series, has an important role in the assessment of the best–fitting curve and of the uncertainty on the corresponding GSLA. F3

To better scrutinize the nature of the non–linear trend shown by the ST curve in Fig. 3, we have compared the results of the quadratic regression, expressed by Eq. (2), with those obtained by a linear and a bi–linear regression, respectively. The adoption of a bi–linear model is motivated by previous studies (e.g. Church and White 2006), which have evidenced the existence of CPs or "inflections" in global sea–level curves, corresponding to abrupt slope variations, hence to short–lived sea–level accelerations. A review of the literature supporting the existence of CPs is given by Gehrels and Woodworth (2013). Furthermore, CPs are also suggested by modeled scenarios of future sea–level rise (Spada et al., 2013), and particularly by the sea–level component expected from terrestrial ice melt, showing abrupt changes of the sea–level trend in response to episodes of enhanced mass loss in Greenland. For the sake of parsimony, we have not attempted to introduce more sophisticated multi–linear regression methods, which appears unmotivated in view of the large errors generally affecting the construction of a global sea–level curve. However, the use of multi–linear models could be appropriate when regional secular sea–level records are considered, as in the case of the Pacific coast of North America (Bromirski et al., 2011).

Here, bi–linear regression has been performed adopting methods employed in econometrics to detect structural changes, i.e. variations of the statistical parameters of non–stationary time series such as ST including, in particular, changes in the rate of variation. The Chow statistics allows for the detection of a CP at a given time (Chow, 1960). In this testing procedure, the time series is split into two sub–periods, and for each of them a linear regression is performed. Continuity is not imposed at the time of occurrence of a CP. The misfit obtained for such bi–linear model is then compared, by means of a Fisher F–test (e.g. Winer 1962), with the one obtained by a linear model for the whole time series. We have implemented the recipe by Hansen (2001), based on an idea of Quandt (1960), which overcomes the limitation caused by the need for the break date to be known *a priori* and introduces a methodology for determining a structural change whose timing is unknown.

Analysis of the ST curve shows that the bi–linear regression significantly improves the fit (at the confidence level $\alpha = 95\%$) with respect to a linear or a quadratic model. The structural CP, which corresponds to the largest value of the Chow statistics, is found within the time interval 1835–1840. This is relatively close to the sea–level acceleration visually evidenced by Jevrejeva et al. (2006) in the period 1850–1870, which appears to be the largest acceleration visible in the sea–level reconstruction during the last 200 years (see their Figure 5). Since the dataset employed and the methods of analysis differ, we tentatively suggest that the CP we have detected effectively corresponds to the acceleration episode described by Jevrejeva et al. (2006). This would constitute, indirectly, a validation of the automated CP search method adopted here. Though the misfit reduction obtained for the bi–linear model is indeed statistically significant (at the 95% significance level) compared to a linear or quadratic regression, the global nature of this CP is dubious. The reason is that only data from six PSMSL stations clustered in Europe contribute to the ST curve in the lapse of time between 1830 and 1849 (namely, Brest (F), Swinoujscie (PL), Sheerness (GB), Cuxhaven 2 (D), Wismar 2 (D), and Maassluis (NL), see Fig. 2b). F2b By similar arguments, Jevrejeva et al. (2006) have pointed to the dubious significance of the acceleration episode, since only five stations, facing the North Atlantic and the Baltic, were in operation. Visual inspection of the six records above corroborate the hypothesis of a CP in the earliest time series (Brest and Swinoujscie), which is also confirmed by a separate analysis. The commencement of the remaining four records around year 1850, followed by a marked and coherent linear sea–level rise, acts to strengthen the 1835–1840 structural change.

To avoid any bias resulting from a poor spatial coverage of the stacked time series, hereinafter we will consider the second branch (referred to as ST2) of ST, pertaining to the time period 1840–2010; this curve is shown in F4 Fig. 4. The number of RLR records that build ST2 progressively increases to $\sim$ 300 until $\sim$ 1960, and decreases to $\sim$ 200 by the year 2010. As we have verified, a sufficient spatial coverage is ensured for the TGs used to construct curve ST2, with no clusterings at continental or regional scales scale during the whole time span. Analysis of curve ST2 reveals that the quadratic regression

$$\mathrm{SL}(t) = (0.0021 \pm 0.0012)\ t^2 + q_1(t), \tag{3}$$

where SL is expressed in mm and t in years and $q_1(t)$ is a linear polynomial, improves the fit ($\alpha = 95\%$) with respect to linear and bi–linear models limited to the same period. Eq. (3) implies an acceleration (0.0042 ± 0.0024) mm/yr^2, which confirms the existence of a GSLA and points, in particular, to the absence of significant CPs during 1840–2011. To test the robustness of these results against the number of TGs used for a given year, we have stacked time series with length ≥ 60 and ≥ 75 years (the number of used TGs reduces from 315 to 225 and 143, respectively). These computations confirm the existence of the GSLA and the absence of significant CPs, showing that Eq. (1) is not introducing artifacts when there is a change in the TGs available at a given time. This has also been confirmed by further computations, in which following Jevrejeva et al. (2006) we have performed the stacking on the rates of each individual time series. The derivatives have been numerically implemented using a two–points, two–sided formula. The resulting sea–level curves essentially reproduce the time–derivatives of our curves ST and ST2, thus showing that no artifacts are introduced when a change in the number of TGs available occurs.

Although the ST2 curve is best–fitted (95%) by a parabola (see Eq. 3), it is of interest to determine the best–fitting bi–linear model. When this is done, the CP is found for year ~ 1940, relatively close to the inflection evidenced by Jevrejeva et al. (2008), Woodworth et al. (2009) and Church and White (2011) for year ~ 1930. For consistency with our statistical approach, this can only be classified as a "weak" CP with low–significance, since the best performing model is, for curve ST2, the quadratic one given by Eq. (3). As pointed by Rahmstorf (2007), the variation of the trend of sea–level rise that occurred in ~ 1940 corresponded to a major variation of the global temperatures. We observe that the GSLA value implied in our estimate (3) turns out to be ~ 3 times smaller than the previous estimate (0.013 ± 0.006 mm/yr^2) by Church and White (2006), which covers a comparable time span, but was obtained by distinct selection criteria and methods of analysis (see Table 1). The precisions of the two estimates, measured by their fractional uncertainty ($\sim 50\%$), are comparable.

2.3. Interpreting the sea–level curve

Averaged expressions like (2) and (3), based on the stacking (1), are appealing, since they are supposed to capture the actual ocean behavior in an apparently simple fashion. However, regardless the averaging methodology adopted, these approaches tend to hide the mechanisms that control the local sea level change recorded in single time series. For instance, the effective source of the quadratic trend itself remains obscure, until the individual components of the stacking are scrutinized or the forcing mechanism is identified. The quadratic growth of curve ST2 does not necessarily imply a similar behavior for all the time series that compose the stack, although one could intuitively expect that a dominance of quadratic time series would be ultimately responsible for the observed GSLA.

To address the issues above, we have classified the 315 TGs that form curves ST and ST2 according to the regression models that best fit each time series that contributes to the stacking. The best fitting models have been determined by ordinary least squares, since serial correlation has been shown by Baki Iz et al. (2012) not to affect the estimates of the trends, while the impact on the uncertainty is minor. With TG–L, TG–Q and TG–B we indicate time series subsets for which the best–fitting statistical model is linear, quadratic and bi–linear, respectively. The performances of these models have been compared analyzing the variances of the residuals by means of a F–test (with $\alpha = 95\%$). The most populated subset is TG–L, which contains 237 time series (75% of the total); most of them (90%) show a positive sea–level trend. Subset TG–Q contains only 47 time series (15% of the total). With the exception of three sites, all the time series belonging to set TG–Q show a positive trend (i.e. the linear term of the quadratic model) and most of them (75%) are characterized by a positive quadratic term (i.e. $a > 0$). Finally, subset TG–B only contains 31 time series ($\sim$ 10% of the total). The CPs of the TG–B time series are marked by vertical bars in Fig. 4, where red and blue colors imply an increase and a decrease of the sea–level trend across the CP, respectively. CPs show a complex temporal distribution, but some patterns emerge. They appear only sporadically before $\sim$ 1960 while they are more frequent and energetic afterwards and particularly during the last four decades. Furthermore, red CPs dominate the blue ones in terms of amplitude and frequency (24 out of the 31 CPs detected are red).

It is worth to recall that the 315 TGs employed to construct curve ST2 were selected only according to the record length criterion. When the analysis performed on the records contributing to ST2 is extended to the D97 (Douglas, 1992) and SG01 (Spada and Galassi, 2012) time series, for which additional selection criteria have been applied, similar results are found. Namely, most of the time series are best–fitted by a linear polynomial (77%

and 81% of the total number of time series for sets D97 and SG01, respectively). The few remaining are almost equally partitioned in two sets, fitted by quadratic and bi–linear models, respectively. This confirms that sets D97 and SG01 are effectively representative of the global set of TGs, also with respect to the style of the statistical models that best–fit their components.

The spatial distribution of TGs belonging to the TG–L, TG–Q and TG–B subsets is shown in Fig. 5. The dominance of positive sea–level trends F5 (red dots) for TG–L stations is apparent in Fig 5a. Negative trends (blue dots) are mainly clustered regionally. These are observed along the North and the South American West coast, where they can be considered, at least partly, as the result of active tectonics along transcurrent and collisional boundaries in these regions. Negative sea–level trends along the Pacific coasts of North America since $\sim$ 1980 have been recently attributed to a steric response to wind stress, and interpreted as indications of an imminent sea–level acceleration (Bromirski et al., 2011). Wind stress has been also recognized as the source of large sea–level drops in the eastern North Pacific and North Atlantic coasts between the late $1800s$ and the early $1900s$ (Sturges and Douglas, 2011). Negative rates of sea–level change observed in northern Europe and particularly along the coasts of the Baltic Sea can be associated with the ongoing post–glacial rebound in response to the melting of the late–Pleistocene ice sheets (see e.g. Spada and Galassi 2012).

Because of their relatively small number compared to TG–L, spatial patterns in the distribution of the TG–Q (Fig. 5b) and of the TG–B TGs (5c) cannot be easily identified. This would suggest that the positive acceleration expected from a stacking of the TG–Q time series does not have a regional origin. It is remarkable that the Japanese TGs show trends of all the three kinds so far discussed. This is likely to reflect the complex tectonic setting of this region (Aubrey and Emery, 1986), which makes the interpretation of the TG signals particularly difficult (see e.g. the discussion in Spada and Galassi 2012). The sea–level time–series for San Francisco falls in the TG–B category (5c). For this record, our analysis indicates a CP for year $\sim$ 1890. According to Bromirski et al. (2011), who limited their attention to the last century, two major discontinuities in the rate of sea–level rise can be evidenced for San Francisco at times $\sim$ 1930 and $\sim$ 1980, which are also visible in the San Diego and Seattle records. In other approaches, based on the smooth Intrinsic Mode Functions (Breaker and Ruzmaikin, 2013), abrupt CPs could not be resolved for the San Francisco record, although their existence is strongly suggested by a visual inspection of the full time series, after the application of a running average filter. Finally, we note that according to our analysis, none of the TGs located in the Pacific area belongs to the TG–B subset. Indeed, application of the "virtual station method" to TG records from this region reveals complex regional patterns that could hardly be consistent with a single–CP regression model (Webb and Kench, 2010).

Using Eq. (1), the time series belonging to the three subsets TG–L, TG–Q and TG–B have been stacked and the resulting global curves have been analyzed in order to determine the best fitting statistical model. This aims F6
to check how different styles contribute to GSLA. The results are shown in Fig. 6. As expected, the stacked TG–L time series are best fitted ($\alpha = 95\%$), by a linear model. Its regression coefficient corresponds to a rate of sea–level rise of (0.94 ± 0.11) mm/yr. Similarly, the stack obtained using TG–Q data are best fitted by a quadratic polynomial that implies a sea–level ac-

celeration (0.003 ± 0.005) mm/yr^2. The stacked TG–B time series, however, demand a quadratic model as well, corresponding to a sea–level acceleration (0.012 ± 0.006) mm/yr^2. For the stacking resulting from the TG–B set, the rejection of a bi–linear model can be interpreted as the cumulative effect of the time sequence of essentially coherent change points that characterize the TG–B time series (their timing and amplitude are shown in Fig. 4). The resulting stacked curve is best–fitted by a parabola characterized by a positive acceleration, matching the envelope of several time series having the shape of linear segments separated by non simultaneous CPs. This is not totally unexpected and was remarked (but not made quantitative) by Gehrels and Woodworth (2013) when discussing the local contribution to global instrumental sea–level curves.

3. Discussion and conclusions

Un–weighted stacking of the longest RLR annual TG time series produces a synthetic global sea–level curve (ST), which shows several features. First, ST shows a statistically significant and positive CP, implying a sudden increase in slope, within the time period 1835–1840. Second, branch ST2 of curve ST, which encompasses the time period 1840–2010, is best fitted by a quadratic polynomial ($\alpha = 95\%$). This confirms previous results about the existence of a GSLA for the period 1840–2010 (Jevrejeva et al., 2006; Church and White, 2006). According to our estimates, the GSLA is (0.0042 ± 0.0024) mm/yr^2. The projection of Eq. (2) to year 2100 suggests a sea–level rise of about 16 cm relative to 1990, at the lower boundary of the IPCC projection for 2100 of the observed sea–level rise from the 20^{th} century, which is in the range of 19-58 cm (Meehl et al., 2007). This estimate would increase to 22 cm using Eq. (2), which represents the best fitting parabola for curve ST (see the supplementary Fig. S1). F1S

The determination of the starting point of the present sea–level rate and acceleration is one of the challenges of current studies since it could unveil correlation with anthropogenic factors or global climate change. The most recent and comprehensive study by Gehrels and Woodworth (2013) has proposed the existence of a possible sea–level inflection at the year 1925 ± 20. This time window includes the early result by Woodworth (1990) who proposed year 1930 for the inflection, which was subsequently confirmed by Church and White (2006) and Woodworth et al. (2009). Since the sea–level curve ST2 is best–fitted by a quadratic model, our statistical analysis does not support the existence of a CP. However, we have verified that among all the possible bi–linear models for ST2, the residues are minimized when a CP at year ~ 1940 is allowed, which could be assimilated to the one evidenced in the previous literature.

Results by Jevrejeva et al. (2006) suggest a major change in the rate of sea–level change during the period 1850–1870, which probably marks the start of present acceleration. Our curve ST evidences a CP between 1835 and 1840 which could be interpreted as a new CP not observed before. It is possible, however, that here we are observing the same short–term acceleration detected Jevrejeva et al. (2006). The non exact temporal coincidence of the two episodes could be justified by the different sets of TGs employed and the different approaches. Furthermore, while in Jevrejeva et al. (2006) the acceleration episode has been identified visually, here we have used an automatic search strategy. Our analysis shows that it is impossible to ascertain the global origin of this CP (or of these CPs), since the few operating

TGs in that period were located in Northern Europe. Similar conclusions have been drawn by Jevrejeva et al. (2006).

The results presented in this work are suggesting a re–evaluation of the same meaning of GSLA. In fact, though the best–fitting model for curve ST2 is indeed quadratic in the time period 1840–2010, our analysis has shown that most of the components follow a linear model. The number of effectively quadratic time series (TG–Q) is limited to $\sim 15\%$ of the total of 315 RLR time series considered in this study. Although the number of bi–linear ones (TG–B) is even smaller ($\sim 10\%$), the time sequence of CPs provides the stack an upward curvature that enhances the effect of the TG–Q time series and coherently emerges from the averaging. One of the reasons the acceleration only emerges in a limited number of sites ($\sim 25\%$) is that long and very long period oscillations dominate the signal while nodal points are scarce and unlikely to coincide with all or just some of the selected observation points.

The findings above, obtained by the application of a modified Chow test (Hansen, 2001), have two important consequences. *i)* when dealing with GSLA, the attribute *global* should be used cautiously, since the vast majority of the TG time series used to construct the ST curve are effectively *not* showing any significant acceleration ($\alpha = 95\%$). Indeed, from an analysis of the distribution of the TG–Q instruments (see Fig. 5), we have found that these are often surrounded by sites that do not show any significant acceleration (see Supplementary Material). The *global* nature of the GSLA only stems from the lack of any apparent regional clustering in the spatial distributions of the TG–Q and TG–B gauges (see Fig. 5), which ultimately determine the parabolic shape of the cumulative curve. *ii)* intermittent and non–synchronous CPs occurring at individual TG since $\sim$ 1880 have an important role in determining an *average* sea–level acceleration on a century time scale. The relevance of "short–term accelerations" enlightened in several previous studies (see Gehrels and Woodworth 2013 and references therein) is therefore confirmed in this study. Here, the problem has been put in a quantitative perspective using statistical methods borrowed from econometrics.

4. Acknowledgments

We are grateful to two anonymous reviewers who have provided very thoughtful comments on a earlier version of the manuscript. We have benefited of some econometrics suggestions from Barbara Petracci and Pierpaolo Pattinoni and of insightful discussions with Fabio Raicich and Florence Colleoni. Sea–level data have been downloaded from the PSMSL (Permanent Service for Mean Sea Level) archive on August 1st, 2012 (*http:// www.psmsl.org /data /obtaining/*). All figures have been drawn using the Generic Mapping Tools (GMT) (Wessel and Smith, 1998).

References

Aubrey, D. G., Emery, K. O., 1986. Relative sea levels of Japan from tide–gauge records. Bull. Geol. Am. Soc. 97, 2, 194–205.

Baki Iz, H., Berry, L., Koch, M., 2012. Modeling regional sea level rise using local tide gauge data. J. Geod. Sci. 2, 3, 188–199.

Bindoff, N., Willebrand, J., Artale, V., Cazenave, A., Gregory, J., Gulev, S., Hanawa, K., Le Quèrè, C., Levitus, S., Nojiri, Y., Shum, C., Talley, L. D., 2007. Observations: oceanic climate change and sea level. In: Solomon, S., Qin, D., Manning, M., Chen, Z., Marquis, M., Averyt, K., Tignor, M., Miller, H. (Eds.), Climate Change 2007:

The Physical Science Basis, Intergovernmental Panel on Climate Change. Cambridge University Press, Cambridge, pp. 385–432.

Breaker, L. C., Ruzmaikin, A., 2013. Estimating rates of acceleration based on the 157–year record of sea level from san francisco, california, u.s.a. J. Coast. Res. 29, 1, 43–51.

Bromirski, P. D., Miller, A. J., Flick, R. E., Auad, G., 2011. Dynamical suppression of sea level rise along the Pacific coast of North America: Indications for imminent acceleration. J. Geoph. Res. 116, C07005.

Carbognin, L., Teatini, P., Tomasin, A., Tosi, L., 2010. Global change and relative sea level rise at Venice: what impact in term of flooding. Clim. Dynam. 35, 6, 1039–1047.

Cazenave, A., Remy, F., 2011. Sea level and climate: measurements and causes of changes. WIREs Clim Change 2, 647–662.

Chambers, D. P., Merrifield, M. A., Nerem, R. S., 2012. Is there a 60–year oscillation in global mean sea level? Geophys. Res. Lett. 39, L18607.

Chow, G. C., 1960. Tests of equality between sets of coefficients in two linear regressions. Econometrica 28, 3, 591–605.

Church, J. A., White, N. J., 2006. A 20th century acceleration in global sea–level. Geophys. Res. Lett. 33, L01602.

Church, J. A., White, N. J., 2011. Sea–level rise from the late 19th to the early 21st century. Survey in Geoph. 32 4, 585–602.

Douglas, B., 1991. Global sea sevel rise. J. Geoph. Res. 96, 6981–6992.

Douglas, B., 1992. Global sea level acceleration. J. Geoph. Res. 97 (C8), 12,699–12,706.

Douglas, B., 1997. Global sea–level rise: a redetermination. Surv. Geophys. 18, 279–292.

Efron, B., Tibshirani, R., 1986. Bootstrap methods for standard errors, confidence intervals, and other measures of statistical accuracy. Statistical Science 1, 54–77.

Gehrels, W. R., Woodworth, P. L., 2013. When did modern rates of sea–level rise start? Global and Planetary Change 100, 263–277.

Gilbert, F., Dziewonski, A., 1975. An application of normal mode theory to the retrieval of structural parameters and source mechanisms from seismic spectra. Phil. Trans. R. Soc. A 278, 187–269.

Gutenberg, B., 1941. Changes in sea level, postglacial uplift and mobility of the Earth's interior. Bull. Geol. Soc. Am. 52, 721–772.

Hansen, B. E., 2001. The new econometrics of structural shange: dating breaks in U.S. labor productivity. Journal of Economic Perspectives 15, 4, 117–128.

Houston, J. R., Dean, R. G., 2013. Effects of sea–level decadal variability on acceleration and trend difference. J. Coast. Res.

Jevrejeva, S., Grinsted, A., Moore, J., Holgate, S., 2006. Nonlinear trends and multiyear cycles in sea level records. J. Geoph. Res. 111, C09012.

Jevrejeva, S., Moore, J. C., Grinsted, A., Woodworth, P. L., 2008. Recent global sea level acceleration started over 200 years ago? Geophys. Res. Lett. 35, L08715.

Larsen, C. F., Echelmeyer, K. A., Freymueller, J. T., Motyka, R., 2003. Tide gauge records of uplift along the northern Pacific–North American plate boundary, 1937 to 2001. J. Geoph. Res. 108 (B4), 2216.

Liu, G., Fomel, S., Jin, L., Chen, X., 2009. Stacking seismic data using local correlation. Geophysics 74, V43–V48.

Meehl, G., Stocker, T., Collins, W., Friedlingstein, P., Gaye, A., Gregory, J., Kitoh, A., Knutti, R., Murphy, J., Noda, A., Raper, S., Watterson, I., Weaver, A., Zhao, Z.-C., 2007. Climate change 2007: The physical science basis, intergovernmental panel on climate change. In: Solomon, S., Qin, D., Manning, M., Chen, Z., Marquis, M., Averyt, K., Tignor, M., Miller, H. (Eds.), Global Climate Projections. Cambridge University Press, Cambridge, pp. 747–845.

Merrifield, M. A., 2011. A shift in western tropical Pacific sea level trends during the 1990s. J. Clim. 24, 15, 4126–4138.

Olivieri, M., Spada, G., Antonioli, A., Galassi, G., 2013. Mazara del Vallo tide gauge observations (1906–1916): land subsidence or sea level rise? Journal of Coastal Research in press.

Peltier, W., 2004. Global glacial isostasy and the surface of the Ice–Age Earth: the ICE–5G(VM2) model and GRACE. Annu. Rev. Earth Pl. Sc. 32, 111–149.

Quandt, R., 1960. Tests of the hypothesis that a linear regression obeys two separate regimes. J. Am. Stat. Ass. 55, 324–330.

Rahmstorf, S., 2007. A semi–empirical approach to projecting future sea–level rise. Science 315, 368–370.

Spada, G., Bamber, J., Hurkmans, R., 2013. The gravitationally consistent sea–level fingerprint of future ice loss. Geoph. Res. Lett. 40 (3), 482–486.

Spada, G., Galassi, G., 2012. New estimates of secular sea–level rise from tide gauge data and GIA modeling. Geophys. J. Int. 191 (3), 1067–1094.

Spada, G., Melini, D., Galassi, G., Colleoni, F., 2012. Modeling sea level changes and geodetic variations by glacial isostasy: the improved SELEN code. http://arxiv.org/abs/1212.5061.

Spada, G., Stocchi, P., 2007. SELEN: a Fortran 90 program for solving the "Sea Level Equation". Comput. and Geosci. 33, 538–562.

Sturges, W., Douglas, B. C., 2011. Wind effects on estimates of sea level rise. J. Geophys. Res. 116, C06008.

Sturges, W., Hong, B., 2001. Decadal variability of sea level. In: Douglas, B., Kearney, M., Leatherman, S. (Eds.), In: Sea level rise, history and consequences. Academic Press, pp. 165–180.

Taylor, J. R., 1997. An introduction to error analysis: the study of uncertainties in physical measurements. University Science Books.

Webb, A. P., Kench, P. S., 2010. The dynamic response of reef islands to sea–level rise: Evidence from multi–decadal analysis of island change in the central pacific. Global Planet. Change 72, 3, 234–246.

Wenzel, M., Schröter, J., 2010. Reconstruction of regional mean sea level anomalies from tide gauges using neural networks. J. Geophys. Res. 115, C08013.

Wessel, P., Smith, W. H. F., 1998. New, improved version of generic mapping tools released. EOS 79, 579.

Winer, B. J., 1962. Statistical principles in experimental design. McGraw–Hill.

Woodworth, P., White, N., Jevrejeva, S., Holgate, S., Church, J., Gehrels, W., 2009. Evidence for the accelerations of sea level on multi–decade and century timescales. Int. J. Climatol. 29, 777–789.

Woodworth, P. L., 1990. A search for accelerations in records of European mean sea level. Int. J. Climatol. 10, 129–143.

Woodworth, P. L., Player, R., 2003. The Permanent Service for Mean Sea Level: an update to the 21st century. J. Coastal Res. 19, 287–295.

Table 1: GSLA estimates based on global analyses of instrumental records, for which a quadratic term in a polynomial regression is evaluated.

Author(s)	year	$a \pm \Delta a$ (mm/yr^2)	Period (year–year)	Input dataset	Methods
Douglas	1992	-0.011 ± 0.012	1905–1985	23 TGs	Averaged group acceleration
” ”	” ”	0.001 ± 0.008	1850–1991	37 TGs	” ”
Church and White	2006	0.013 ± 0.006	1870–2001	PSMSL TGs	EOFs
” ”	” ”	0.008 ± 0.008	20^{th} century	” ”	” ”
Jevrejeva et al.	2008	~ 0.01	1700–2002	1023 RLR PSMSL TGs	Virtual station method
Church and White	2011	0.009 ± 0.003	1880–2009	PSMSL TGs and NASA/CNES altimetry	EOFs
This study	2013	0.0098 ± 0.0023	1820–2010	315 PSMSL RLR TGs	Stacking (ST curve)
This study	2013	0.0042 ± 0.0024	1840–2010	” ”	Stacking (ST2 curve)

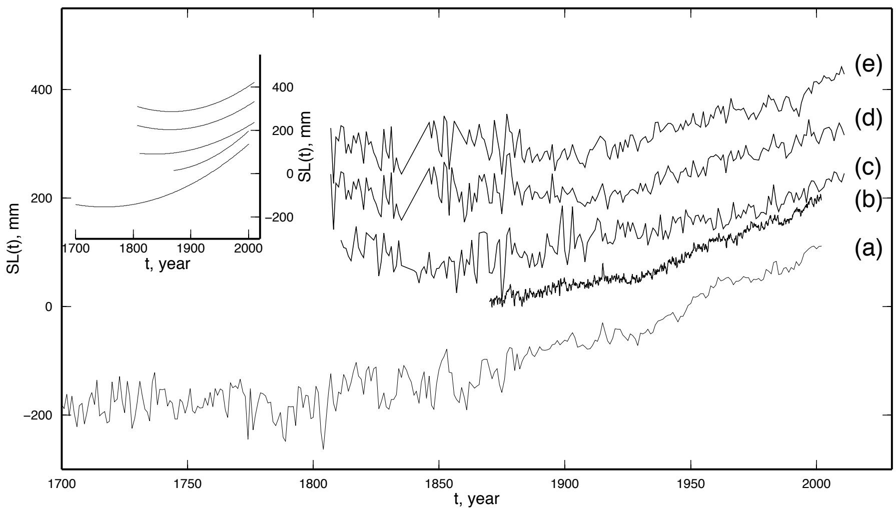

Figure 1: Various sea–level curves relevant to this work (the curves are shifted by an arbitrary amount for to facilitate visualization). Curves (a) and (b) show the reconstructions by Jevrejeva et al. (2006) (the standard errors are not reproduced from the original work) and Church and White (2006), respectively. Curve (c) is the ST time series obtained in this work by the stacking of RLR TG observations. Curves (d) and (e) result from the stacking of the TGs selected by Douglas (1992) and by Spada and Galassi (2012). The best–fitting quadratic polynomials to curves (a–e) are shown in the inset, while numerical values of the corresponding accelerations are given in Table 1.

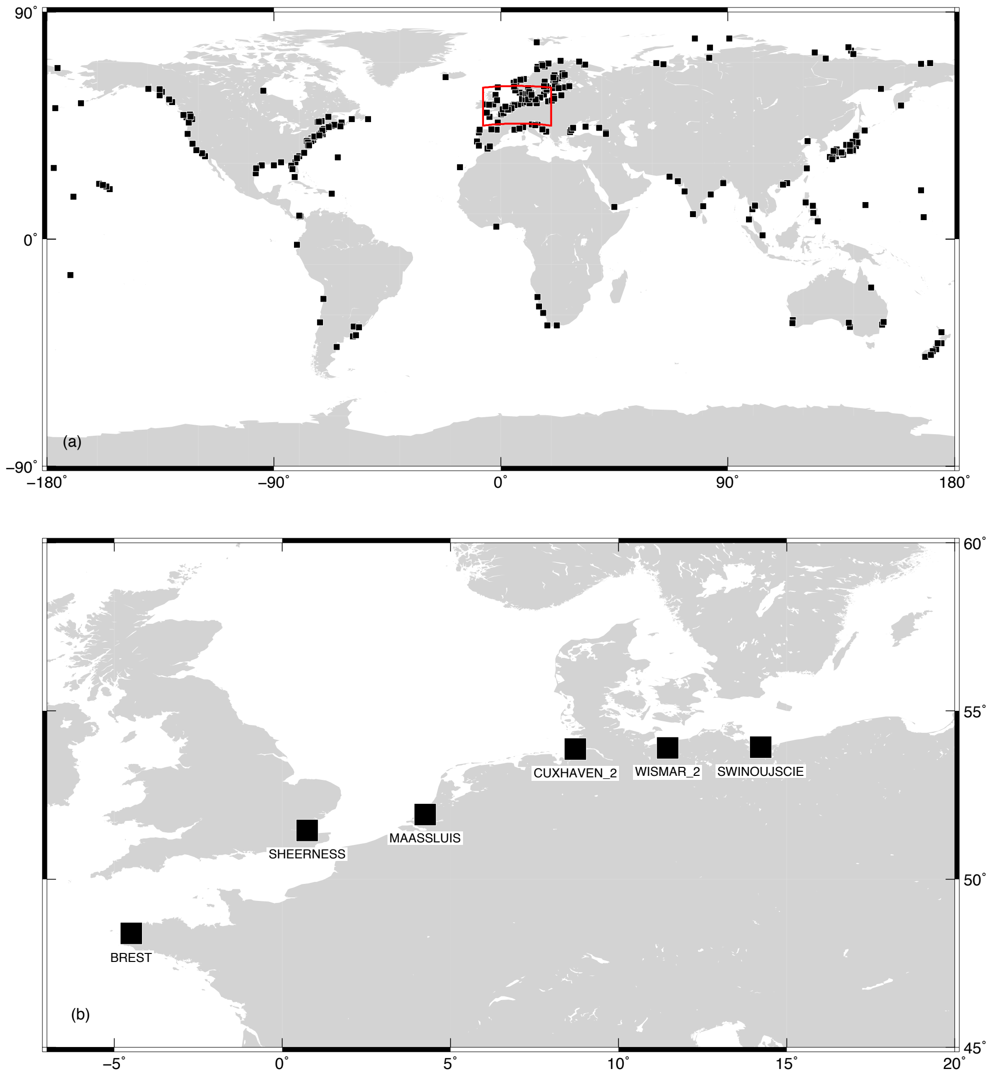

Figure 2: (a) Geographical distribution of the 315 RLR TGs for which > 50 years of data are available within the period 1820–2010, which build the ST curve. The region in the inset is enlarged in (b), and shows the location of the six North European TG rime series available in the period 1830–1849.

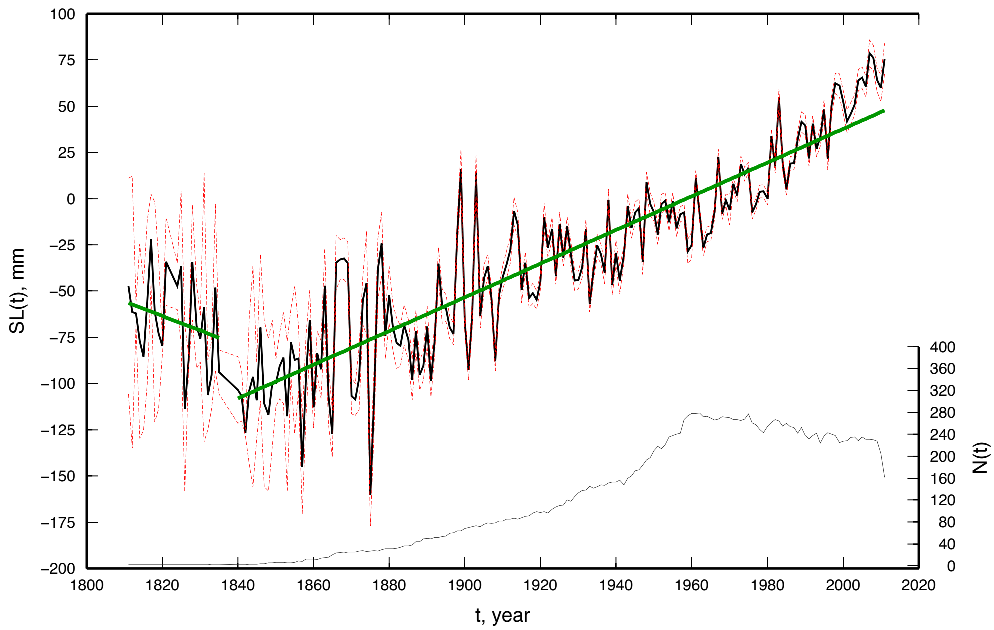

Figure 3: The stacked curve ST (black), obtained from Eq. (1) for the period 1810–2010 and the range of uncertainty corresponding to SLD(t_i) (red). The green line represents the best fitting bi–linear model for ST, showing a CP for year 1835–1840. The regression coefficient rises from (-1 ± 3) mm/yr before the CP to (0.91 ± 0.05) mm/yr after the CP. The plot at the bottom shows $N(t)$, the number of time series available in the stacking at a given epoch t.

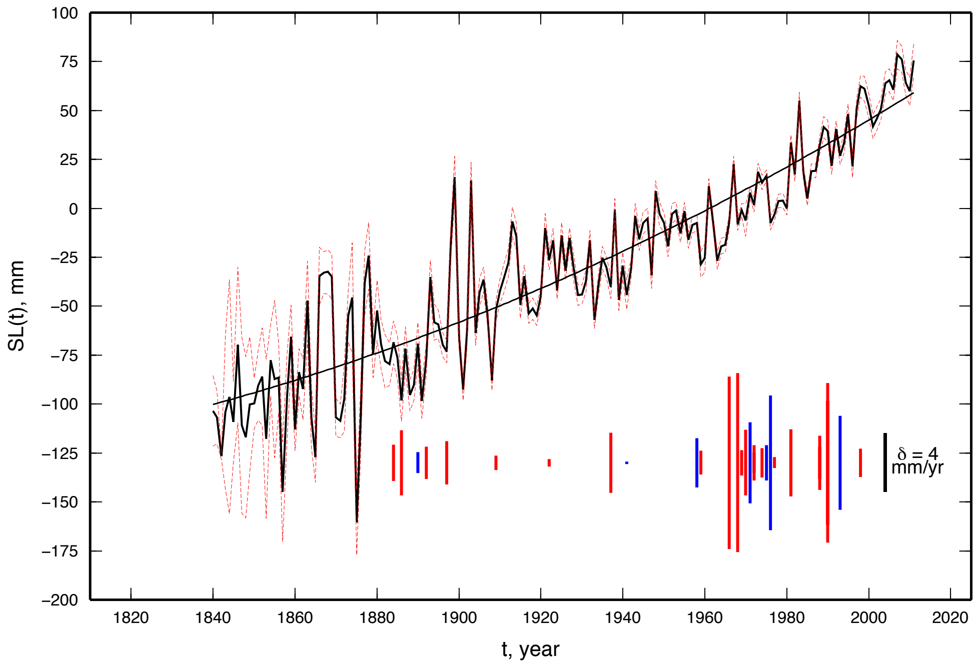

Figure 4: The same as in Fig. 3, but for curve ST2, obtained from Eq. (1) for the period 1840–2010. The black curve shows the best fitting quadratic polynomial. Vertical bars at the bottom of figure show the sequence of CPs found for each of the time series in the TG–B set. Red and blue segments indicate CPs for which the variation in the rate of sea–level change, denoted by δ, is positive and negative, respectively.

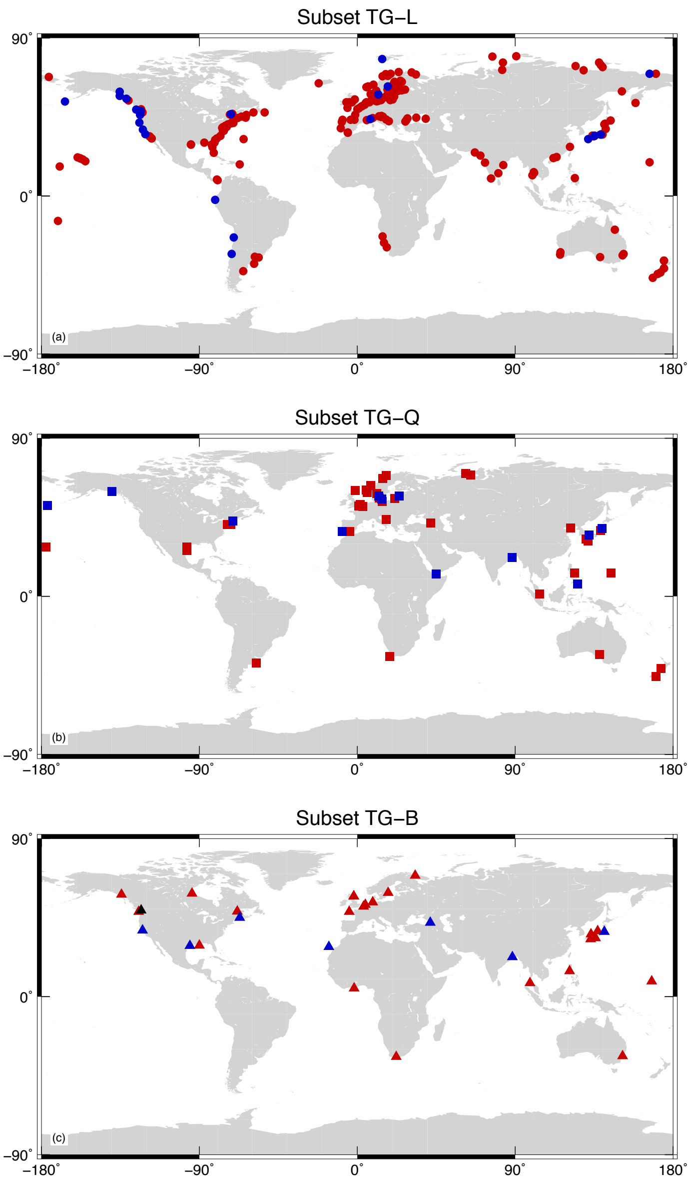

Figure 5: Locations of TGs according to the best–fitting model. (a): Subset TG–L (red and blue symbols denote positive and negative trends, respectively), (b): TG–Q (the red color indicates a positive quadratic term, the blue a negative one), (c): TG–B (red and blue colors indicate positive and negative values of δ (see Fig. 4).

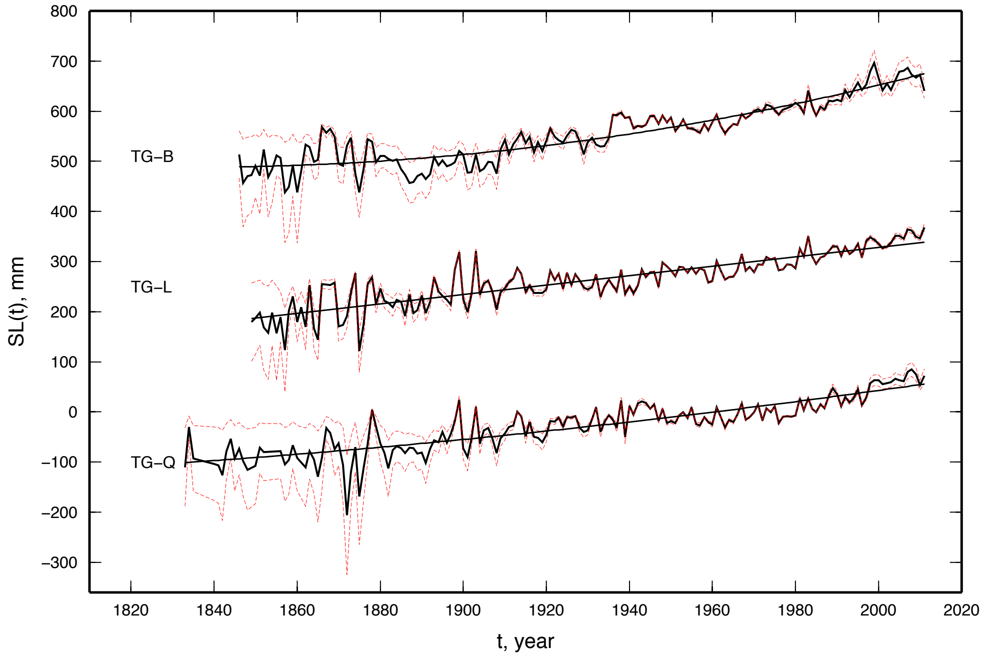

Figure 6: Stacking obtained for the time series belonging to the TG–B (top), TG–L (middle) and the TG–Q (bottom) subsets. For the three subsets, the best fitting models are quadratic, linear and quadratic, respectively. Red dashed curves mark the 1σ interval for the stacks.